UNCLASSIFIED

SPECinc stratton park engineering company inc cloud physics and instrumentation

"Characterization of Aerosol Inlets and Ducts"
Topic No. N01-047
Phase II Proposal Plan

R. Paul Lawson, Principal Investigator

SPEC, Inc.
3022 Sterling Circle, Suite 200
Boulder, CO 80301

Contract No. N00014-01-M-0122
Office of Naval Research

2 October 2001

NOTE: Approved for public release; SBIR report, distribution unlimited.

UNCLASSIFIED

20011005 366

1. Results of the Phase I Research

The research conducted in Phase I led to the design and laboratory testing of a device that aids in the evaluation of the efficiency of aerosol inlets. The device will be tested in Phase II on a research aircraft by comparing the particle size distribution measured by a forward scattering spectrometer probe (FSSP) in the aerosol inlet with an FSSP mounted on the wing. **Figure 1** shows a Solidworks™ drawing and a photograph of the inlet calibration device. Laboratory tests showed that the device reliably measures the size distribution of glass beads in a predictable airflow through the FSSP sample volume.

2. Phase II and Phase I → II Transition Objectives

2.1 Phase II Technical Objectives

1. Modify the laboratory version of the aerosol inlet calibration device designed in Phase I for application on a research aircraft. Build two inlet calibration devices (one for flight tests with the SPEC Learjet and another for the Navy Twin Otter) and perform additional laboratory experiments with an FSSP-300.

2. Install a standard diffuser aerosol inlet on the SPEC Learjet

3. Design and fabricate a new airborne dual-imaging probe for measuring particles from about 5 to 1000 μm in size.

4. Equip the SPEC Learjet with an FSSP and the new dual-imaging probe installed in the wingtips, and an FSSP with the aerosol inlet calibration device installed in the cabin.

5. Evaluate the performance of the aerosol inlet calibration device by flying the specially equipped Learjet in atmospheres laden with large aerosols.

6. Analyze the data collected by the Learjet research aircraft and write the final report.

2.2 Phase I → II Transition Technical Objectives

During the four-month transition period between Phase I and Phase II, we will complete Solidworks™ mechanical and Zemax™ optical designs for inlet calibration devices for the additional three conductive tubing diameters commonly used in aerosol measurements. We will begin to design the inlet(s) to be installed on the SPEC Learjet research aircraft and work with Navy personnel to determine the best way to adapt the inlet calibration devices for use on the Navy Twin Otter. The diffuser inlet for the Learjet will be designed and engineering for FAA approval will be initiated. We will also begin to design the new 2D-S imaging probe and finalize the engineering parameters for ordering the custom 128-photodiode array.

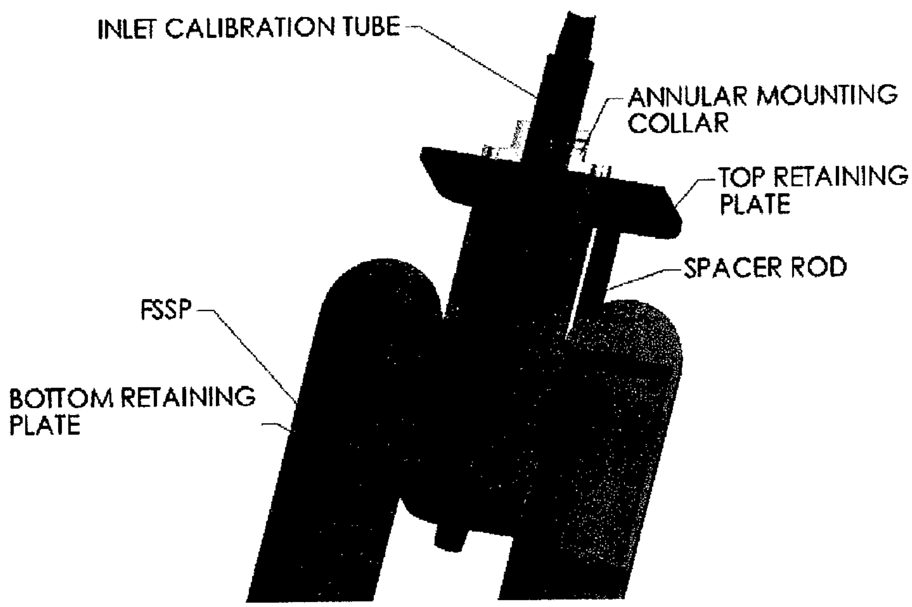

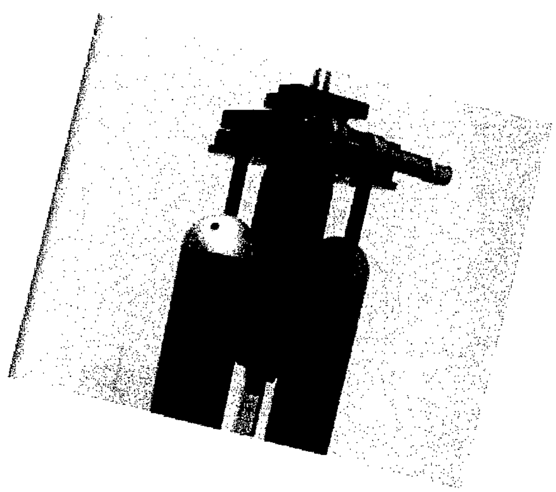

Figure 1. Solidworks drawing (top) of the inlet calibration device and a photograph showing the actual device built in Phase I.

3. Phase II Research Plan

3.1 Modify the Inlet Calibration Device and Perform Additional Laboratory Experiments

A minor modification will be performed to the current design of the inlet calibration device. The lip of the device has been machined to a very sharp edge to reduce flow distortion. Since the laboratory device was machined out of aluminum for ease of manufacture, it can easily be damaged or deformed in the lip region. In Phase II, we will manufacture *two* inlet calibration devices (one for testing on the Lear and one for the Navy to use on the Twin Otter) out of stainless steel so that the thin-walled lip is not easily damaged.

The inlet calibration device was evaluated in Phase I using an FSSP-100. The first one or two bins in the lower size ranges (i.e., range 2 and 3) of the FSSP-100 are known to respond to aerosols and are also noisy. Because of this, we were only able to start collecting usable data starting from about 2 μm. In Phase II, we will borrow an FSSP-300 from the National Center for Atmospheric Research (NCAR) in order to evaluate the inlet calibration device using aerosols in the 1 to 5 μm size range. Glass beads, such as used in Phase I, clump together when one attempts to introduce beads in the 1 to 5 μm size range into the sample volume of an FSSP. Instead of glass beads, we will use aerosols with a known size distribution for laboratory tests with the FSSP-300. To generate the aerosols, we plan to lease a TSI aerosol generator or lease time at the Colorado State University (CSU) Cloud and Aerosol Simulation Laboratory.

3.2 Install a Standard Diffuser Inlet on the SPEC Learjet

A standard diffuser type aerosol inlet will be installed under the fuselage of the Learjet research aircraft. The inlet will have a straight manifold section with nozzles for connections to the FSSP. The manifold will then be exhausted to the airstream at the back of the cabin of the Lear.

3.3 Two-dimensional Particle Imaging (2D-S) Probe

The FSSP-100 used to measure the size of glass beads during the Phase I research measures aerosols and cloud particles in the 3 to 45 μm size range, however, the sampling statistics for the larger (10 to 45 μm) size particles are poor due to the small sample volume. This is an inherent limitation of single-particle scattering devices such as the FSSP and the phase Doppler particle analyzer (PDPA) (Bachalo and Houser 1984).

In order to improve the sampling statistics for aerosols in the 10 to 300 μm size range, a new optical imaging device will be fabricated in Phase II for application on the research aircraft. The new probe will image particles as small as 5 to 10 μm and have more than ten times the sample volume of the FSSP. The probe, called a 2D stereo (2D-S) probe, will provide stereo images of particles with a minimum size of 5 to 10 μm. This will cover the larger aerosol size range as well as the small cloud particle size range, including small ice particles and drizzle drops.

Errors due to electro-optical limitations that are inherent in the design of the PMS 2D-C probe have been well documented in the literature. Korolev et al. (1991, 1998) have shown that large counting and sizing uncertainties occur with the PMS 2D particle imaging probes when particles pass outside the optical depth of field (DOF). **Figure 2** is an adaptation from Korolev et al. (1998) and illustrates the sizing and counting errors associated with the PMS 2D-C probe. The illustration shows that as particles < 150 μm are imaged outside of the DOF, the digitized image diffraction pattern initially gets larger, creating oversizing errors, and then eventually fragments so that the image size is much less than the actual size. At some distance from the center of the DOF, the particle image disappears all together. In this case, the particle images are not detected at all. The effective size of the DOF is governed by the relationship DOF = cr^2/λ (Knollenberg 1970), where r is the particle radius, λ is the wavelength of incident light and c is a constant, which was measured by Knollenberg to be equal to about 6 for a shadow depth of 40%. Thus, the DOF gets larger as a function of the square of the particle size, until at $r = \sim 75$ μm it reaches the physical boundaries of the probe arms. However, for a small particle with a diameter of 20 μm, the DOF is about 1 mm, or 1/60th of the distance between the probe arms.

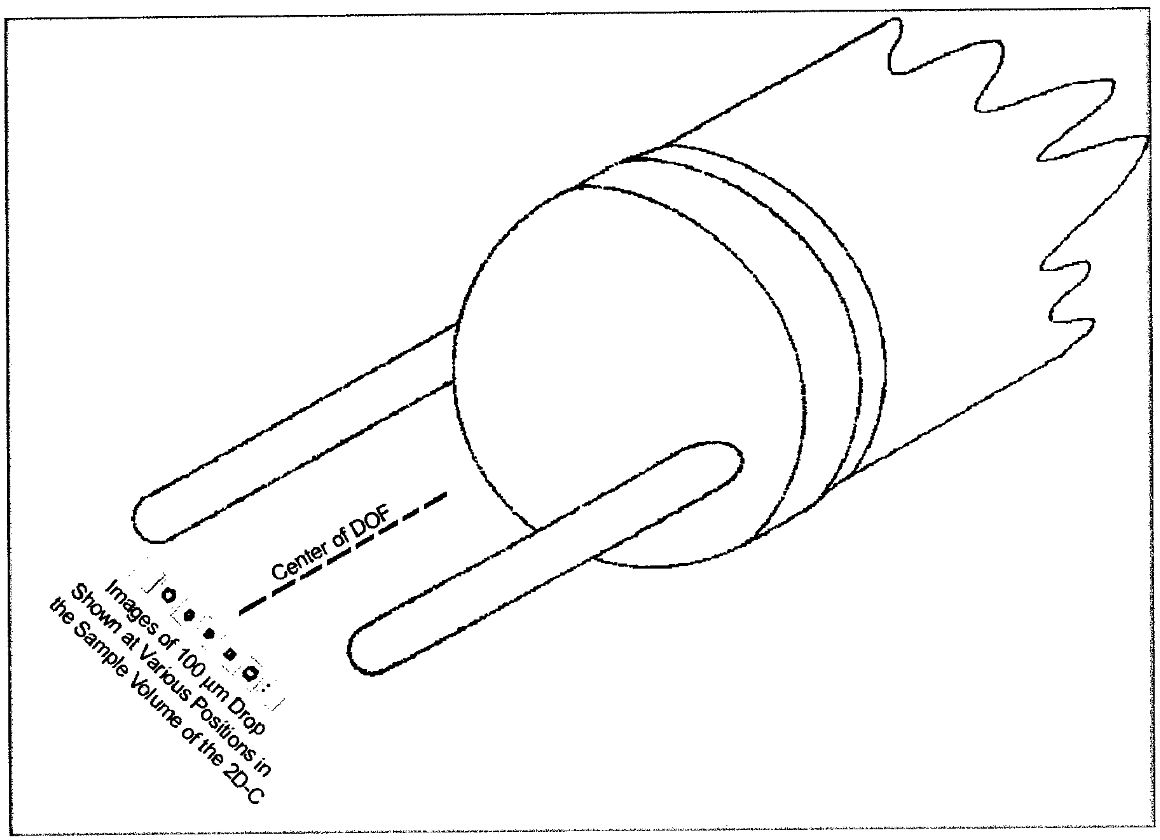

Figure 2. Illustration showing how the digital image of a 100 μm circular particle will appear to get larger, then much smaller, and eventually disappear as the particle moves from the center of the DOF toward the 2D-C probe tips (images from digitized diffraction simulations found in Korolev et al. 1998).

In addition to the sizing and counting errors associated with particles passing outside the optical DOF, additional errors occur in the PMS 2D-C probe as a result of the finite time response of the photodiode array and first stage amplifier. Baumgardner and Korolev (1997), and more recently Strapp et al. (2001), show that the limited time response of the PMS imaging probes is limited by the time constant of the photodiode array and first stage amplifier, leading to a significant reduction in sensitivity to small (< ~100 μm) particles. For example, laboratory results reported by Strapp et al. (2001) in **Figure 3** show that at an airspeed of 100 m s^{-1} the effective DOF is reduced by nearly an order of magnitude for 60 μm particles, and that 20% of 60 μm particles that pass directly through the center of the DOF are not detected at all.

A new probe, called a 2D-S (stereo) probe, will be built in Phase II. A conceptual drawing illustrating the functional aspects of the 2D-S probe is shown in **Figure 4**. The 2D-S will record simultaneous stereo images of particles. The new electro-optics will essentially eliminate the uncertainties associated with particles passing outside the optical DOF, and will also will have sufficient time response to detect particles < 10 μm at an airspeed > 100 m s^{-1}. As shown in **Figure 4**, two diode lasers will illuminate two linear 128-photodiode arrays that are situated at right angles to one another. Particles will be sized simultaneously by both linear 128-photodiode arrays. A schematic of the 2D-S probe showing how the dual photodiode array configuration will precisely define the sample volume and virtually eliminate sizing and counting errors due to out of focus particles is shown in **Figure 5**. The laser beams cross at right angles and precisely define a rectangular region in the middle of the probe. Since both optical paths have an associated DOF, the overlap to these DOFs defines a region within which all particles will be in focus that are larger than a predetermined size.

The DOF can be determined by setting the threshold of the shadow depth. Korolev et al. (1998), in their Figure 13, show theoretical relationships between shadow intensity and particle size. From this figure, which shows the maximum DOF for an ideal probe with infinite pixel resolution, the DOF for a shadow depth of 75% (25% in the Korolev et al. figure) is about 3 r^2/λ. An actual probe with finite pixel size will have a slightly smaller DOF, perhaps 2 r^2/λ. The 2D-S probe can be designed so that the DOF for the smallest particles of interest and the overlap region of the two laser beams coincide. Consider the following example that is based on a 128-photodiode array with 10 μm pixel resolution, which would correspond to a rectangular sample area of about 1.3 mm by 1.3 mm. Such a configuration would be adequate for cloud particles and very large aerosols. With a shadow depth set at 80%, each linear array will have a DOF that is ~1.5 mm for particles with diameters of about 40 μm. **Figure 5a** shows an example of a small (say 25 μm) particle in the overlap region and the signals produced on each linear array.

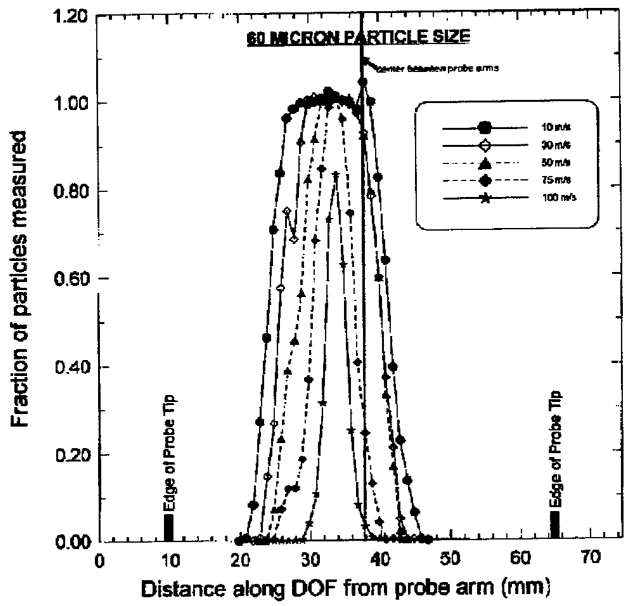

Figure 3. Measured response of a 2DC probe, as a function of velocity, to a constant stream of 60 µm particles across the entire length of the exposed laser. Plotted is a fraction of particles measured as a function of distance from the inside position of the laser side probe arm. The zero area images (ZAIs) are included.

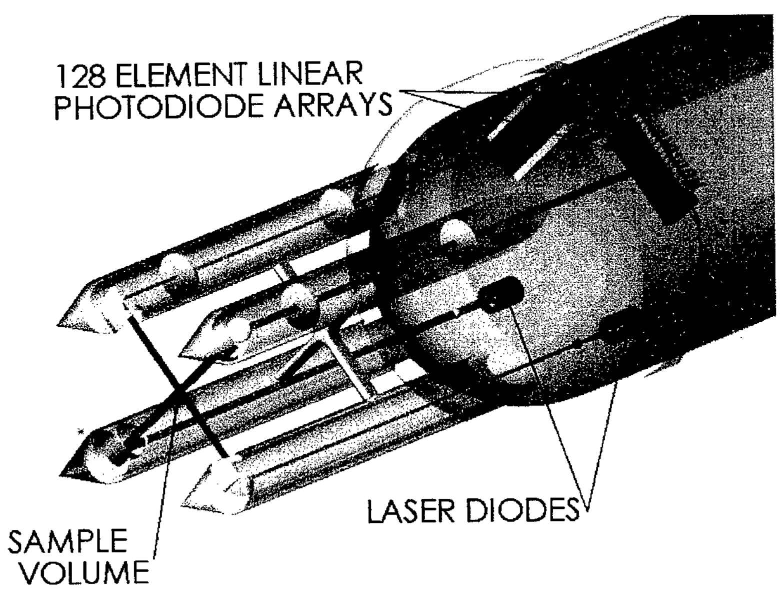

Figure 4. Conceptual solidmodel of a 2D stereo probe. Two laser systems will illuminate two linear 128-photodiode arrays. The sample volume is shown where the two laser beams intersect at 90°.

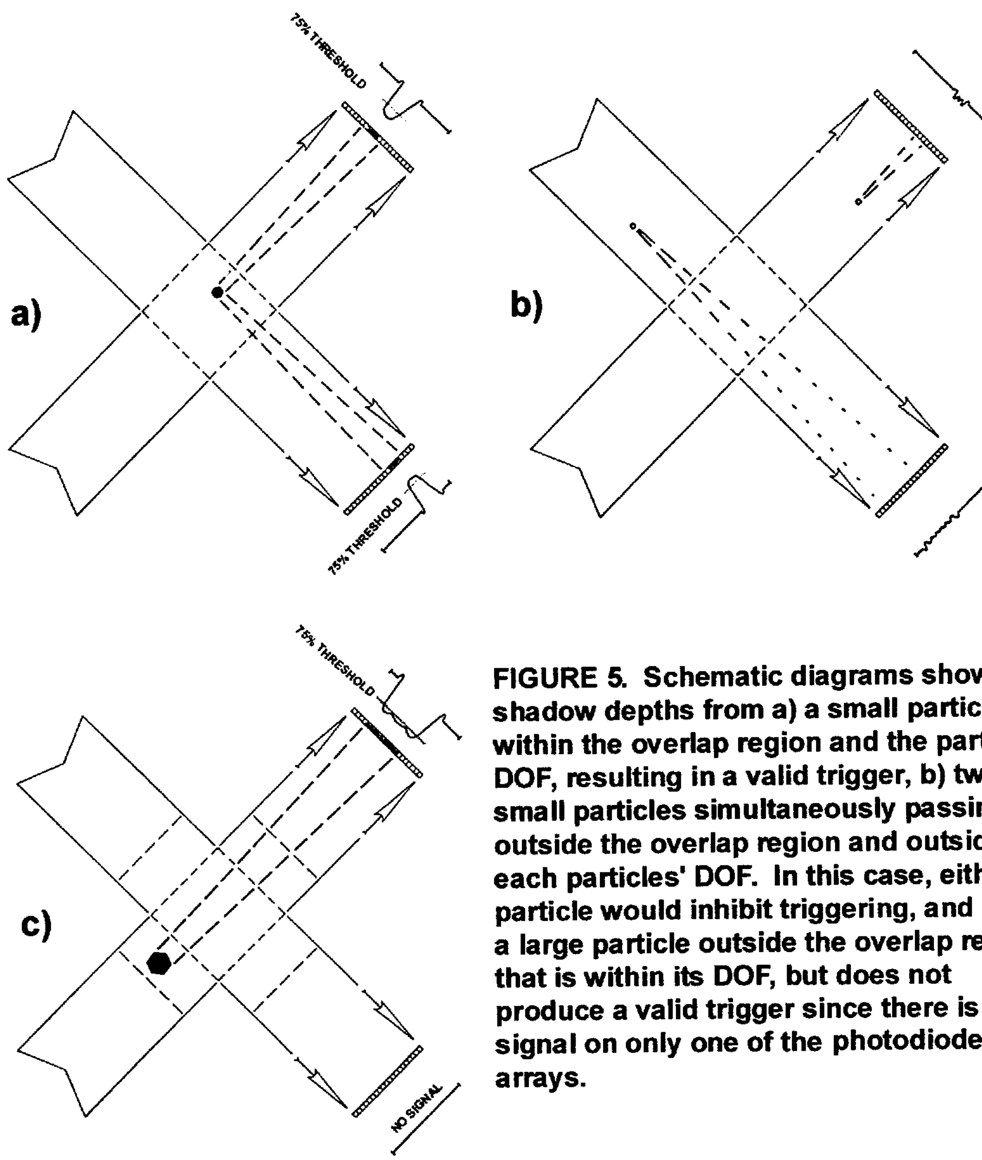

FIGURE 5. Schematic diagrams showing shadow depths from a) a small particle within the overlap region and the particle's DOF, resulting in a valid trigger, b) two small particles simultaneously passing outside the overlap region and outside each particles' DOF. In this case, either particle would inhibit triggering, and c) a large particle outside the overlap region that is within its DOF, but does not produce a valid trigger since there is a signal on only one of the photodiode arrays.

Small particles that are outside the overlap region of the PDS system will generate a shadow depth that is too shallow to exceed the threshold level (**Figure 5b**). This is important, because otherwise, high concentrations of small particles would still cause triggering due to coincidence in the regions where the laser beams do not overlap. Large particles that pass outside the laser beam overlap region will produce a shadow with sufficient depth to register on only one array (**Figure 5c**). However, this will not produce a valid signal since the 2D-S probe can be programmed to only accept particles that register simultaneously on both arrays. Also, since larger particles are found in lower concentrations, the probability will be low that two larger particles will pass simultaneously through the non-overlap regions of the laser beams. The 2D-S probe could also be configured for smaller (aerosol) particles. For example, a 128-photodiode array with 5 μm pixel resolution is possible; however, the time constant of the photodiode array and first stage amplifier will be the critical design factor limiting sensitivity to small particles.

In order to substantially increase the time response of the photodiode array and first stage amplifier, a new 128-element linear photodiode array will be custom built by United Detector Technology (UDT) Corporation. In order to substantially reduce the time constant of the electro-optics, UDT will incorporate 128 op-amps into the substrate of the photodiode array. This is the only way to significantly increase the response time of the array, which is otherwise limited by the capacitance in the photodiodes and the circuit board traces that lead to the first-stage amplifier. Droplet Measurement Technologies (DMT) has improved the speed of conventional photodiode arrays to the practical limit, which has decreased the time constant of the array and first-stage amplifier from about 0.4 μs to about 0.25 μs. The new hybrid photodiode/op-amp array will achieve a time constant < 0.1 μs, possibility as fast as 0.05 μs, thereby facilitating the detection of 5 to 10 μm particles at an airspeed of 100 m s^{-1}.

The 2D-S probe will also be programmed so that the user can select the particle size at which the imaging system is triggered. For example, if measurements are being made in new cumulus to search for first ice, the probe can be configured to "fish" for particles (i.e., ice crystals) that are larger than 50 μm by only triggering on particles that occult more than four photo diodes (~48 μm). Another feature that will be incorporated into the probe is the ability to recognize "stuck bits" due to optical contamination, streakers or noise. The stuck bits will be "masked" (i.e., ignored) in much the same way that the SPEC HVPS masks stuck bits.

3.4 Flight Test the Inlet Calibration Device and 2D-S probe

The SPEC Learjet will be used to evaluate the airborne performance of the inlet calibration device and the 2D-S probe. **Figure 6** shows photographs of the SPEC Learjet and sensors. The FSSP and 2D-S probes will be installed in the wingtip locations and the diffuser inlet will be installed under the fuselage. The windstorms that occur in the lee of the Rocky Mountains, scouring the plains and sending large dust particles several thousands of feet into the atmosphere.

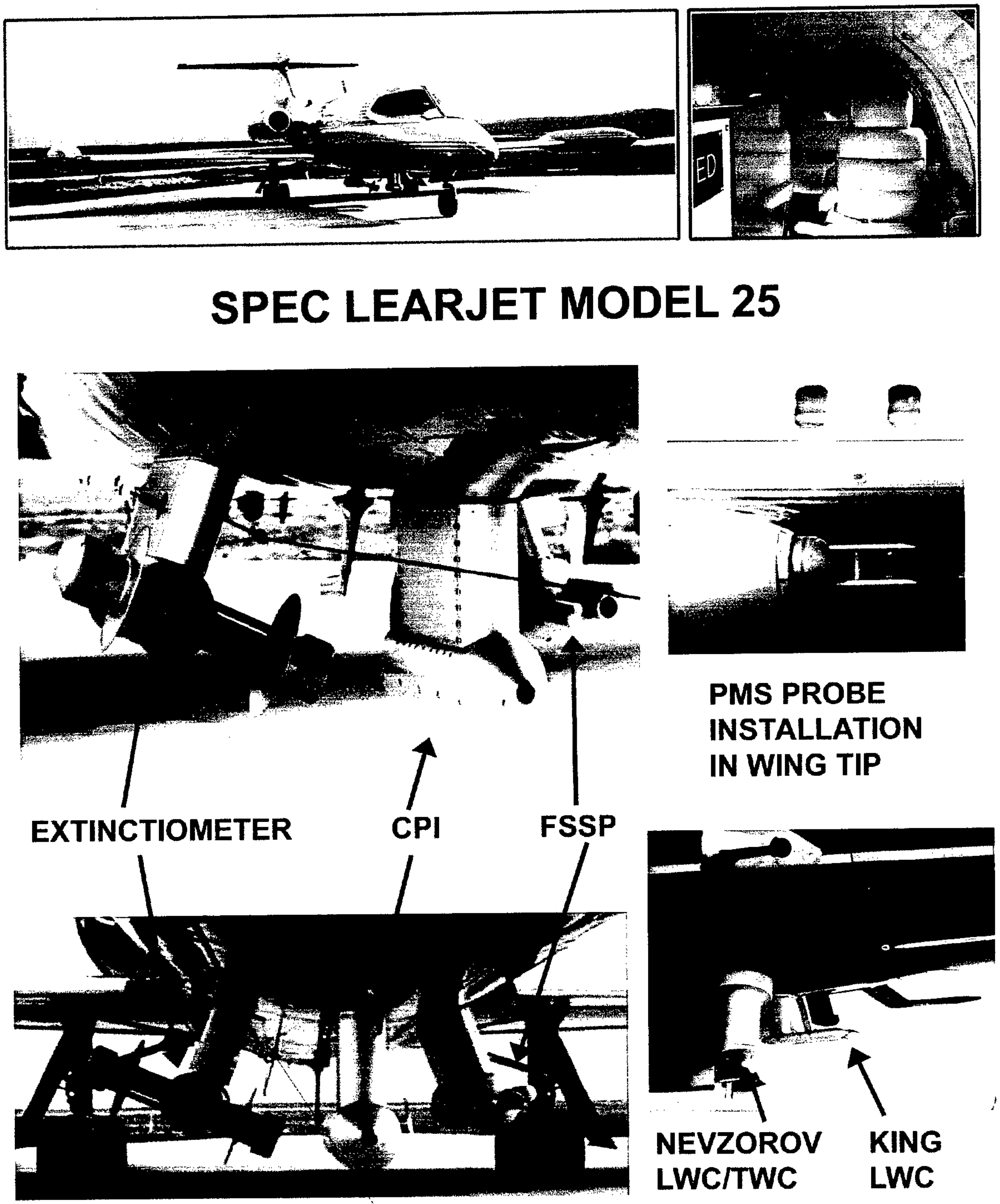

Figure 6. Photographs of the SPEC Learjet showing the interior and sensor locations.

3.5 Analyze the Flight Data and Write the Final Report

Results from the laboratory experiments and data collected by the SPEC Learjet will be analyzed in Phase II. The final report will include a comprehensive analysis of the performance of the inlet calibration device and the 2D-S probe.

References

Bachalo, W.D. and M.J. Houser, 1984: Phase/Doppler spray analyzer for simultaneous measurements of drop size and velocity distributions. *Optical Eng.,* **23,** 583-590.

Baumgardner, D. and A. Korolev, 1997: Airspeed corrections for optical array probe sample volumes. *J. Atmos. Oceanic Technol.,* 14, 1224-1229.

Knollenberg, R.G., 1970: The optical array: An alternative to scattering or extinction for airborne particle size determination. *J. Appl. Meteor.*, **1(1)**, 86-103.

Korolev, A. V., S. V. Kuznetsov, Y. E. Makarov, and V. S. Novikov, 1991: Evaluation of measurements of particle size and sample area from optical array probes. *J. Atmos. Oceanic Technol.,* **8,** 514-522.

Korolev, A.V., J.W. Strapp and G.A. Isaac, 1998: Evaluation of the Accuracy of PMS Optical Array Probes. *J. Atmos. Oceanic Technol.*, **15**, 708-720.

Strapp, J.W., F. Albers, A. Reuter, A.V. Korolev, U. Maixner, E. Rashke and Z. Vukovic, 2001: Laboratory Measurements of the Response of a PMS OAP-2DC. *J. Atmos. And Oceanic Technol.*, **18 (7)**, 1150-1170.